

# UV Radiation Curing of Surface Coatings Based on ENR-Cycloaliphatic Diepoxyd-Glycidyl Methacrylate System by Cationic Photoinitiators-Optimization of Process Variables Through Response Surface Methodology

R.N. Kumar, Woo Choon Kong, and Abusamah Abubakar—Universiti Sains Malaysia\*

## INTRODUCTION

The coatings industry has been seeking alternative technologies that are less polluting than the currently employed solvent-based systems that cause the emission of volatile organic compounds (VOCs) during curing. The technologies based on ultraviolet (UV) radiation and electron beam (EB) curing are ideally suited to meet the stringent environmental regulations curtailing the VOC emissions. There has been a growing interest in recent years in the cationically initiated photopolymerization due to the development of very efficient photoinitiators and to the distinct advantages of this method of radiation curing. Monomers that are inactive with free radicals, such as epoxides or lactones, as well as conventional monomers like vinyl ethers, can be polymerized in the presence of sulphonium salts. However, resin systems employed in cationic curing are all petroleum derived and must be exclusively imported into Malaysia. With a goal of finding an alternative raw material based on a renewable resource, investigations were initiated in our laboratory to employ epoxidized natural rubber (ENR) for the purpose.

Besides providing a strong economic incentive, ENR can impart toughness to the cured epoxide systems. It is well known that small amounts of elastomer can greatly improve the fracture resistance or toughness of epoxy resins by forming discrete rubbery domains. These elastomeric domains can be chemically bonded to the matrix for high efficiency. The coating system used for our studies consisted of a cycloaliphatic diepoxyd (3,4 epoxycyclohexylmethyl-3,4-epoxycyclohexane carboxylate), ENR (ENR 50, which is a 50 mole percent epoxidized natural rubber), and glycidyl methacrylate (GMA). Preliminary studies<sup>1</sup> showed that the cured film had a two-phase morphology with the ENR remaining in the elastomeric domain and thereby contributing to the toughness of the cured coating. GMA, on the other hand, functioned as a crosslinking agent by providing the dual reactive sites, namely the glycidyl and acrylic groups. The acrylic double bonds of the latter can react with the residual isoprene double bonds of the ENR while the epoxy groups enter into a copolymerization reaction with the epoxy groups of the ENR and cycloaliphatic diepoxyd thereby producing an interpenetrating poly-

*This paper reports on the results of the ultraviolet curing of surface coatings based on cycloaliphatic diepoxyd-epoxidized natural rubber (ENR)-glycidyl methacrylate (GMA) system with a cationic photoinitiator. The results reported in our earlier publication<sup>1</sup> showed that ENR acts as a toughening agent for the otherwise brittle epoxy resin, and that GMA functions as a crosslinking agent in the system and promotes adhesion between the elastomeric domain and the resin matrix. In this paper, the results of the effect of operating variables on the properties of the cured film are reported. Response surface methodology (RSM) was employed to collect data and to establish the functional relationships between operating variables and performance characteristics of the cured coatings. The data are represented in three-dimensional response surface plots. These plots not only enable the interpretation of results, but also allow the determination of the optimum treatment combinations required to maximize the properties of the surface coatings.*

mer network. The presence of GMA thus ensures and promotes adhesion between the elastomeric domain and the epoxy resin. The results of these preliminary studies encouraged us to pursue further an in-depth evaluation of the properties of the cured coatings under different operating conditions. This was considered important since the coatings have to meet rigorous appearance and physical property standards. Coating systems such as the one used for our studies are inherently complex in

\*Wood Paper and Coatings Div., School of Industrial Technology, 11800 Pulau Pinang, Malaysia.

**Table 1—Design Matrix for Central Composition Design**

Run No.	$x_1$	$x_2$	$x_3$	$x_4$	$x_5$
1	n = $2^{k-1}$ where k = 5 .....	1	1	1	-1
2	Fractional factorial design .....	1	-1	-1	-1
3	.....	-1	1	-1	-1
4	.....	-1	-1	1	-1
5	.....	1	-1	1	1
6	.....	-1	-1	-1	1
7	.....	-1	1	1	-1
8	.....	1	1	-1	1
9	.....	-1	-1	1	1
10	.....	1	-1	1	-1
11	.....	-1	-1	-1	1
12	.....	-1	1	-1	1
13	.....	1	1	1	1
14	.....	1	1	-1	1
15	.....	1	-1	-1	1
16	.....	-1	1	1	-1
17	Axial or star points .....	2	0	0	0
18	.....	-2	0	0	0
19	.....	0	2	0	0
20	.....	0	-2	0	0
21	.....	0	0	2	0
22	.....	0	0	-2	0
23	.....	0	0	0	2
24	.....	0	0	0	-2
25	.....	0	0	0	0
26	.....	0	0	0	-2
27	Design centerpoints .....	0	0	0	0
28	.....	0	0	0	0
29	.....	0	0	0	0
30	.....	0	0	0	0
31	.....	0	0	0	0
32	.....	0	0	0	0

nature. Therefore they should be studied with methodologies that will demonstrate unambiguously not only the influence of process variables but also potential interactions between the ingredients and the operating variables. Statistically designed experiments fulfill this requirement and give the significant product improvements with far less effort than is required for conventional study. Reviews of recent coating literature have demonstrated the increased use of statistics in the design and analysis of experiments.<sup>2-6</sup>

### Statistical Experiment Approach

Statistically designed experiments offer a potential solution to the previously mentioned problems and allow coatings chemists the opportunity to work with many factors and responses in a single design. Well-designed experiments yield much more information than conventional experimentation with far less effort and vastly reduced risks in developing conclusions. Several

design types have been applied to the development of coating formulations ranging from factorial design and mixture experiments to Taguchi experiments and central composite designs.<sup>3</sup>

Response surface methodology (RSM) has been widely used in the empirical study of the relationship between one or more measured responses such as yield and color index, on one hand, and a number of input variables such as time, temperature, pressure, and concentration on the other hand.<sup>7</sup>

The objective of statistical experimentation is to establish the functional relationship between a response and a set of factors of interest to the process technologist. This is accomplished by constructing a model that describes the response over the applicable ranges of the factors of interest. This fitted model is referred to as the response surface because the response can be graphed as a curve in two dimensions or a surface in three dimensions. The response surface can be explored to determine important characteristics such as optimum operating conditions.

An equally important reason for fitting and studying the response surfaces is the determination of response sensitivity of a response to various factors. Another use of response-surface design is to find factor regions that produce the best combination of several different responses.

In the case of UV-curable surface coating systems, non-linear trends in the response are likely and hence a second-order polynomial model could be considered to fit adequately the experimental results.<sup>1</sup> An efficient class of experimental designs known as central composite design (CCD) is used to generate data that will fit in the second-order response surface. The basic central composite design for k variables consists of a  $2^k$  factorial design with each factor at two levels (-1, +1) superimposed on a star design or  $2^k$  axial points and several repetitions at the design center points.

Five process variables which are most likely to affect properties of cured films produced from the ENR-50/Epoxy/GMA hybrid system were identified and investigated by a central composite rotatable design. These variables were: (1) ENR 50 to epoxy mixing ratio, (2) photoinitiator percentage, (3) UV exposure time before post cure, and (4) post-cure time and post-cure temperature.

Because a large number of variables have been included in the present studies, a fractional factorial design was adopted as the core of the design to reduce the number of experiments. The experimental design matrix in coded variables is given in Table 1.

**Table 2—Relationship Between Coded and Real Values**

Factors	Coded Levels/Real Levels				
	-2	-1	0	1	2
ENR 50 ratio (phr) .....	$x_1$	10	15	20	25
Photoinitiator percentage (%) (Triphenyl sulfonium hexafluoro antimonate) .....	$x_2$	1	2	3	4
UV exposure time (sec) .....	$x_3$	5	10	15	20
Post-cure time in oven (min) .....	$x_4$	10	20	30	40
Post-cure temperature in oven (°C) .....	$x_5$	80	90	100	110
					120

Table 3—Experimental Data

R	Coded Variables & Levels					Responses		
	X1	X2	X3	X4	X5	Hardness (s) (Pendulum)	Flexibility (mm-1) (Mandrel)	Gel Content (%)
1	1	1	1	-1	-1	129	0.0833	97.37
2	1	-1	-1	-1	-1	61	1.0000	95.83
3	-1	1	-1	-1	-1	145	0.0500	97.55
4	-1	-1	1	-1	-1	116	0.1667	100.32
5	1	-1	1	1	-1	139	0.2000	98.04
6	-1	-1	-1	1	-1	131	0.2500	97.61
7	-1	1	1	1	-1	160	0.0400	99.89
8	1	1	-1	1	-1	169	0.0769	95.03
9	-1	-1	1	1	1	151	0.0526	98.10
10	1	-1	1	-1	1	113	0.2000	100.62
11	-1	-1	-1	-1	1	119	0.1667	97.93
12	-1	1	-1	1	1	161	0.0625	98.81
13	1	1	1	1	1	162	0.0500	98.09
14	1	1	-1	-1	1	159	0.1667	97.40
15	1	-1	-1	1	1	123	0.3333	94.22
16	-1	1	1	-1	1	158	0.0769	99.53
17	2	0	0	0	0	153	0.0769	96.98
18	-2	0	0	0	0	151	0.0500	98.63
19	0	2	0	0	0	160	0.0769	98.31
20	0	-2	0	0	0	114	0.1667	98.03
21	0	0	2	0	0	192	0.0313	98.96
22	0	0	-2	0	0	116	0.2000	93.42
23	0	0	0	2	0	154	0.0625	98.12
24	0	0	0	-2	0	144	0.0625	99.12
25	0	0	0	0	2	159	0.0313	98.59
26	0	0	0	0	-2	148	0.0526	97.58
27	0	0	0	0	0	157	0.0500	99.67
28	0	0	0	0	0	156	0.0500	97.96
29	0	0	0	0	0	152	0.0526	98.67
30	0	0	0	0	0	156	0.0500	99.39
31	0	0	0	0	0	157	0.0500	98.62
32	0	0	0	0	0	156	0.0526	99.21

The coded values in the design matrix of *Table 1* correspond to the following values that the two factors could take for this particular design in a specified region of factor space:

Lowest value	$-\alpha$
Low value	$-1$
Middle value	$0$
High value	$+1$
Highest value	$+\alpha$

Where  $\alpha = (nj)^{1/4}$ ,  $nj = 2^k$  for full factorial design and  $nj = 2^{k-1}$  for a half-replicate of a factorial design, and  $k$  = number of factors. The relationship between the coded and the real variables is given in *Table 2*.

Two different ranges of post-cure time and post-cure temperature were explored in the present study. Initially the range for post-cure temperature was fixed in the interval 80 to 120°C, and the range for the post-cure time was adopted in the interval of 10 to 50 min. The results, however, indicated that both of the post-cure temperature and post-cure time ranges can be reduced so that the conditions of cure are less stringent and more favorable for high productivity.

## EXPERIMENTAL

### Materials

The following were used in this work:

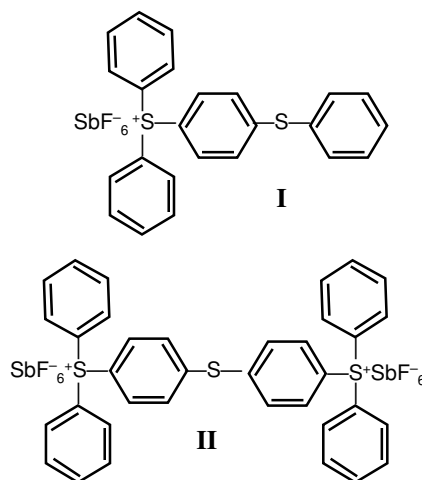
(1) Epoxidized natural rubber (ENR) used in the present work was Epoxyrene, which was 50 mole per-

cent epoxidized. This material was obtained from Guthrie Chemara, Seramban, Malaysia.

(2) The cycloaliphatic epoxide resin employed in the present work as 3,4-epoxycyclohexylmethyl-3,4-epoxycyclohexane carboxylate (Degacure™ KI 85) from Degussa AG, Germany.

(3) Glycidyl methacrylate (GMA) was of BDH grade obtained from Fluka Chemie AG, Buchs, Switzerland.

(4) The cationic photoinitiator employed in this work was Cyracone™ UVI 6974 from Union Carbide Chemicals and Plastics, Danbury, CT, USA. It is a 50% solution in propylene carbonate of two hexafluoroantimonates, I and II, having the following structures:



## Methods

Coatings were formulated according to the conditions stipulated in the prescribed design and coated (40  $\mu\text{m}$ ) on 120  $\times$  70 mm aluminum plate and silicone backed release paper. Three responses were tested: pendulum hardness, mandrel flexibility, and gel content. Pendulum hardness was determined according to DIN 53157. Mandrel flexibility was determined by the ASTM D 1737 test method. Gel content was determined by extraction with hot toluene in a Soxhlet extraction apparatus as described by Du Cong et al.<sup>8</sup>

Experiments were conducted in accordance with the design matrix given in *Table 1*. In this table the various treatment combinations are furnished in coded variables in accordance with the usual practice of statistical design of experiments.<sup>9</sup> The relationship between the coded and real variables is given in *Table 2*. From *Tables 1* and *2*, the actual quantities used in each formulation can be determined. The results of hardness, flexibility, and gel content are presented in *Table 3*.

## RESULTS AND DISCUSSION

The analysis of the results of the experimental data tabulated in *Table 2* were carried out by Statgraphic Version 5 Software (Statistical Graphics System by Statistical Graphics Corp.). The analyses led to the following:

(1) Estimation of regression coefficients of the polynomial equation representing the response surface.

(2) Construction of the analysis of variance (ANOVA) table to determine the significance of the first degree, second degree, and cross-product terms of the polynomial.

(3) The plotting of the response surfaces geometrically so that the dependence of the properties of the UV-cured coatings on the process variables is visually represented. This in turn makes interpretation of data and

**Table 4—Regression Coefficients for Pendulum Hardness**

Constant	=	157.523
A:ENR50	=	-3.41667
B:PI	=	15.9167
C:UV	=	8.83333
D:Post-time	=	9
E:Post-temperature	=	4.91667
AB	=	4.75
AC	=	0.125
AD	=	4.125
AE	=	1.375
BC	=	-6.875
BD	=	-4.625
BE	=	-1.375
CD	=	-0.25
CE	=	-1
DE	=	-6.25
AA	=	-2.77273
BB	=	-6.52273
CC	=	-2.27273
DD	=	-3.52273
EE	=	-2.39773

**Table 5—Regression Coefficients for Mandrel Flexibility**

Constant	=	0.0331659
A:ENR50	=	0.0541083
B:PI	=	-0.0809417
C:UV	=	-0.0655833
D:Post-time	=	-0.0352083
E:Post-temperature	=	-0.0333667
AB	=	-0.0593625
AC	=	-0.0531625
AD	=	-0.0459125
AE	=	-0.0288875
BC	=	0.06405
BD	=	0.034376
BE	=	0.060625
CD	=	0.029775
CE	=	0.033575
DE	=	0.038825
AA	=	0.0208466
BB	=	0.0354341
CC	=	0.0338966
DD	=	0.0206091
EE	=	0.0154716

development of physical insight into the process mechanism easier to visualize.

The regression coefficients of the second degree polynomial relating pendulum hardness, mandrel flexibility, and gel content with various process variables are given in *Tables 4* to *6* and the corresponding analyses of variance are given in *Tables 7* to *9*.

Only those regression coefficients for which the F ratios exceed the  $F_{0.05}(1,11) = 4.84$  were considered significant enough to be included in the polynomials, and the rest of the coefficients were omitted from the response function. Based on the ANOVA, the final regression equations involving pendulum hardness, mandrel flexibility, and gel content are given in the following:

$$\text{Pendulum Hardness}—y = 157.523 + 15.9167x_2 + 8.83333x_3 + 9x_4 - 6.52273(x_2)^2$$

$$\text{Mandrel Flexibility}—y = 0.0331659 + 0.0541083x_1 - 0.08094x_2 - 0.65583x_3 + 0.06405x_2x_3$$

$$\text{Gel Content}—y = 98.8457 - 0.685x_1 + 1.19417x_3 - 0.365x_4 + 0.3562x_1x_3 + 0.4187x_2x_4 - 0.36x_4x_5 - 0.60818(x_3)^2$$

**THE RESPONSE SURFACE PLOTS:** A series of three-dimensional plots is presented in *Figures 1* to *11*. In these plots each of the response variables (pendulum hardness, flexibility, and gel content) is plotted on the z-axis against process variables taken two at a time along the x and y axes in each figure. From the pictorial representation of the variations, it is easy to visualize the effect of operating variables and to interpret the results. Since the number of operating variables is five, there are 10 response plots for each operating variable. It is however, considered unnecessary to furnish all the surface plots. Only a few representative plots which are essential for the interpretation of the results have been given.

The effect of operating variables on pendulum hardness in the three-dimensional plots and the effect of ENR content on hardness can be observed in *Figures 1* to *4*. It can be seen that the hardness decreases as the ENR

**Table 6—Regression Coefficients for Gel Content**

Constant	=	98.8457
A:ENR50	=	-0.685
B:PI	=	0.065
C:UV	=	1.19417
D:Post-time	=	-0.365
E:Post-temperature	=	0.211667
AB	=	-0.165
AC	=	0.35625
AD	=	-0.3075
AE	=	0.31625
BC	=	-0.3375
BD	=	0.41875
BE	=	0.3075
CD	=	-0.0425
CE	=	-0.10125
DE	=	-0.36
AA	=	-0.204432
BB	=	-0.113182
CC	=	-0.608182
DD	=	-6.81818E-4

Table 7—ANOVA for Pendulum Hardness—5 Factor Study

	Sum of Squares	DF	Mean Sq.	F-Patio	P-value
A:ENR50	280.16667	1	280.1667	1.14	.3077
B:PI	6080.16667	1	6080.1667	24.83	.0004
C:UV	1872.66667	1	1872.6667	7.65	.0184
D:Post-time	1944.00000	1	1944.0000	7.94	.0167
E:Post-temperature	580.16667	1	580.1667	2.37	.1520
AB	361.00000	1	361.0000	1.47	.2501
AC	.25000	1	.2500	.00	.9754
AD	272.25000	1	272.2500	1.11	.3143
AE	30.25000	1	30.2500	.12	.7356
BC	756.25000	1	756.2500	3.09	.1066
BD	342.25000	1	342.2500	1.40	.2621
BE	30.25000	1	30.2500	.12	.7356
CD	1.00000	1	1.0000	.00	.9509
CE	16.00000	1	16.0000	.07	.8056
DE	625.00000	1	625.0000	2.55	.1385
AA	225.51515	1	225.5152	.92	.3679
BB	1248.01515	1	1248.0152	5.10	.0453
CC	151.51515	1	151.5152	.62	.4564
DD	364.01515	1	364.0152	1.49	.2483
EE	168.64015	1	168.6402	.69	.4330
Total error	2693.90152	11	244.9001		
Total (corr). ....	17627.7187	31			
R-squared = 0.847178					
R-squared (adj. for d.f.). .... = 0.56932					
F ( $\alpha$ ) 1,11 = 4.84 where $\alpha$ = 0.05, and					
(a) x represents significant factors or interaction of factors.					

Table 8—ANOVA for Mandrel Flexibility—5 Factor Study

	Sum of Squares	DF	Mean Sq.	F-Patio	P-value
A:ENR50	.07026508	1	.0702651	5.51	.0387
B:PI	.15723728	1	.1572373	12.33	.0049
C:UV	.10322817	1	.1032282	8.10	.0159
D:Post-time	.02975104	1	.0297510	2.33	.1549
E:Post-temperature	.02672003	1	.0267200	2.10	.1756
AB	.05638250	1	.0563825	4.42	.0593
AC	.04522002	1	.0452200	3.55	.0864
AD	.03372732	1	.0337273	2.65	.1321
AE	.01335180	1	.0133518	1.05	.3281
BC	.06563844	1	.0656384	5.15	.0444
BD	.01890625	1	.0189063	1.48	.2488
BE	.05880625	1	.0588063	4.61	.0549
CD	.01418481	1	.0141848	1.11	.3142
CE	.01803649	1	.0180365	1.41	.2593
DE	.02411809	1	.0241181	1.89	.1964
AA	.01274769	1	.0127477	1.00	.3493
BB	.03683019	1	.0368302	2.89	.1173
CC	.03370338	1	.0337034	2.64	.1323
DD	.01245888	1	.0124589	.98	.3545
EE	.00702152	1	.0070215	.55	.4813
Total error	.14025124	11	.0127501		
Total (corr). ....	.95604632	31			
R-squared = 0.853301					
R-squared (adj. for d.f.). .... = 0.586575					
F ( $\alpha$ ) 1,11 = 4.84 where $\alpha$ = 0.05, and					
(a) x represents significant factors or interaction of factors.					

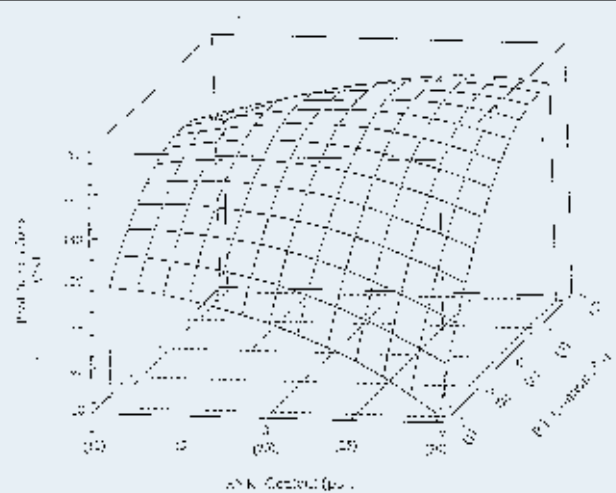


Figure 1—Response surface plot of pendulum hardness as a function of ENR content (phr) and photoinitiator concentration (%). Values in the parentheses are the real values.

content increases under all conditions. This is expected since ENR is flexible and can impart toughness to the intrinsically brittle epoxy coating. While achieving increased toughness, it is generally inevitable that there is a trade off in film hardness. While optimizing the conditions for desired coating performance, a compromise is generally reached between hardness and toughness depending on the end application by adjusting the quantity of elastomer in the formulation and controlling the other operating variables. This can be carried out by plotting responses as contours, choosing the most appropriate values of responses, and determining the values of operating variables to produce the desired response.

Table 9—ANOVA for Gel Content—5 Factor Study

	Sum of Squares	DF	Mean Sq.	F-Patio	P-value	
A:ENR50	11.2614000	1	11.261400	29.55	.0002	x <sup>a</sup>
B:PI	.1014000	1	.101400	.27	.6210	
C:UV	34.2248157	1	34.224817	90.11	.0000	x
D:Post-time	3.1974000	1	3.197400	8.42	.0144	x
E:Post-temperature	1.0752667	1	1.075267	2.83	.1206	
AB	.4356000	1	.435600	1.15	.3071	
AC	2.0306250	1	2.030625	5.35	.0411	x
AD	1.5129000	1	1.512900	3.98	.0713	
AE	1.6002250	1	1.600225	4.21	.0647	
BC	1.8225000	1	1.822500	4.80	.0509	
BD	2.8056250	1	2.805625	7.39	.0200	x
BE	1.5129000	1	1.512900	3.98	.0713	
CD	.0289000	1	.028900	.08	.7907	
CE	.1640250	1	.164025	.43	.5314	
DE	2.0736000	1	2.073600	5.46	.0394	x
AA	1.2259095	1	1.225909	6.23	.0999	
BB	.3757636	1	.375764	.99	.3517	
CC	10.8499636	1	10.849964	28.57	.0002	x
DD	.0000136	1	.000014	.00	.9954	
EE	.5301095	1	.530109	1.40	.2623	x
Total error	4.1777530	11	.379795			

R-squared = 0.847178

R-squared (adj. for d.f.) ..... = 0.56932

F ( $\alpha$ ) 1,11 = 4.84 where  $\alpha$  = 0.05, and

(a) x represents significant factors or interaction of factors.

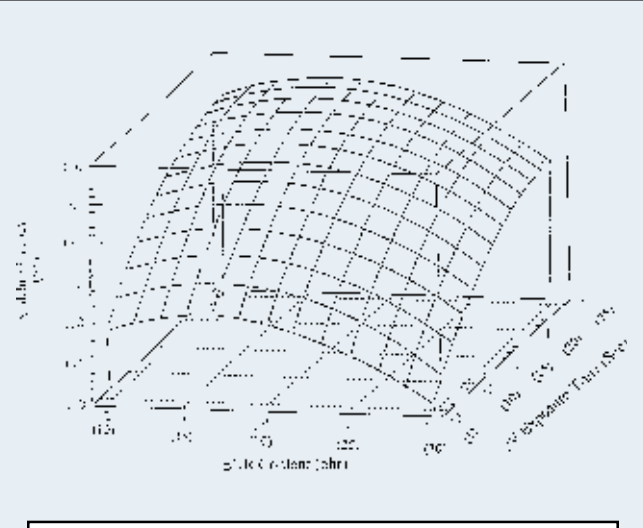


Figure 2—Response surface plot of pendulum hardness as a function of ENR content (phr) and UV exposure time (sec). Values in the parentheses are the real values.

The effects on film hardness with photoinitiator concentration (PI), UV exposure time, post-cure time, and post-cure temperature are shown in Figures 1 to 4.

It can be seen from Figure 1 that the hardness values increase initially as the photoinitiator concentration increases and then levels off. This is expected since the rate of polymerization and crosslinking are proportional to the initiator concentration.<sup>10</sup> A similar trend has been observed by Crivello et al.<sup>11</sup> However, as the photoinitiator concentration is further increased, there is an additional effect due to the plasticizing tendency of the photolytic products of the sulphonium salts as reported by Udagawa et al.<sup>12</sup> Another possibility might be due to the recombination in the “cage” of the free radicals that

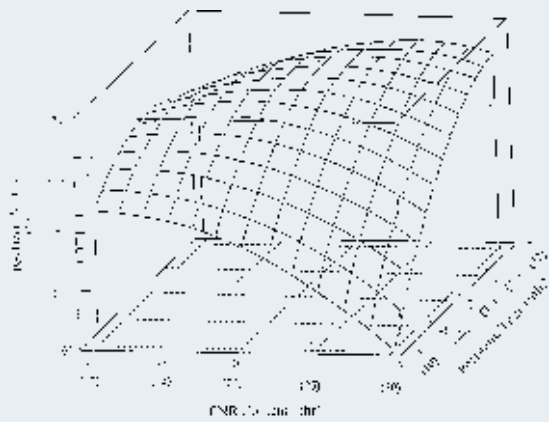


Figure 3—Response surface plot of pendulum hardness as a function of ENR content (phr) and post-cure time (min). Values in the parentheses are the real values.

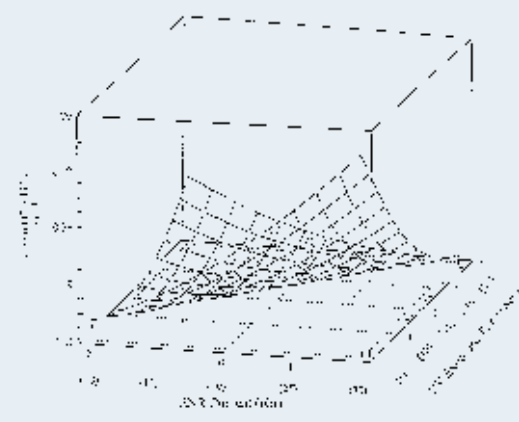


Figure 6—Response surface plot of mandrel flexibility as a function of ENR content (phr) and UV exposure time (sec). Values in the parentheses are the real values.

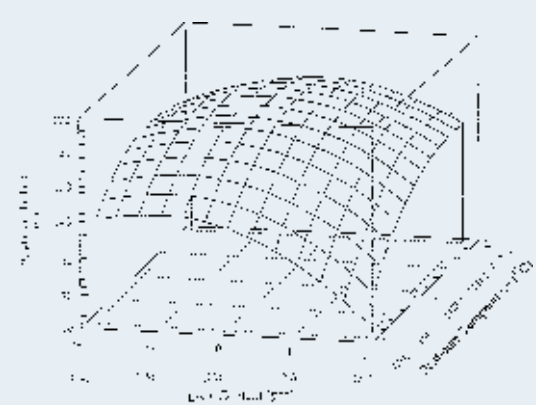


Figure 4—Response surface plot of pendulum hardness as a function of ENR content (phr) and post-cure temperature (°C). Values in the parentheses are the real values.

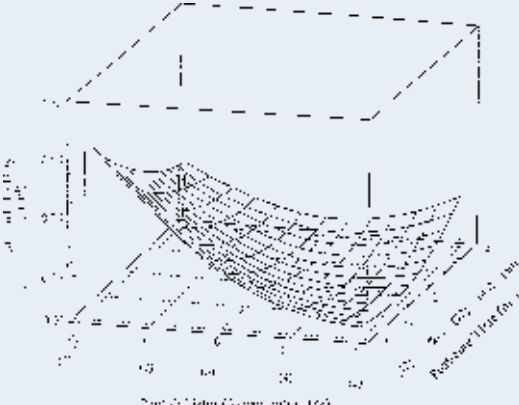


Figure 7—Response surface plot of mandrel flexibility as a function of photoinitiator concentration (%) and post-cure time (min). Values in the parentheses are the real values.

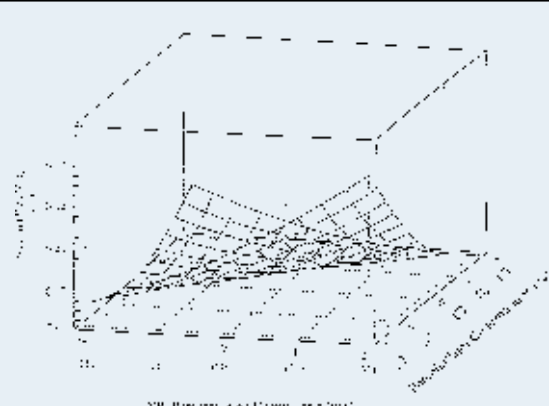


Figure 5—Response surface plot of mandrel flexibility as a function of ENR (phr) and the photoinitiator concentration. Values in the parentheses are the real values.

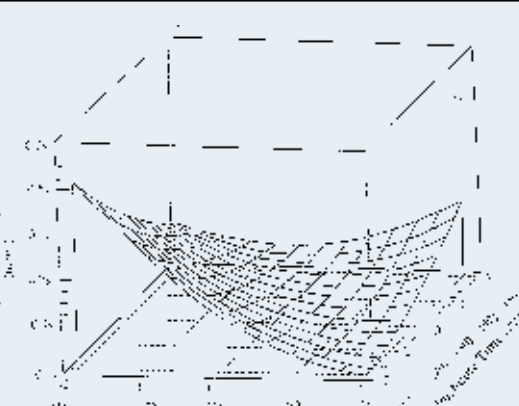


Figure 8—Response surface plot of mandrel flexibility as a function of photoinitiator concentration and post-cure time (min). Values in the parentheses are the real values.

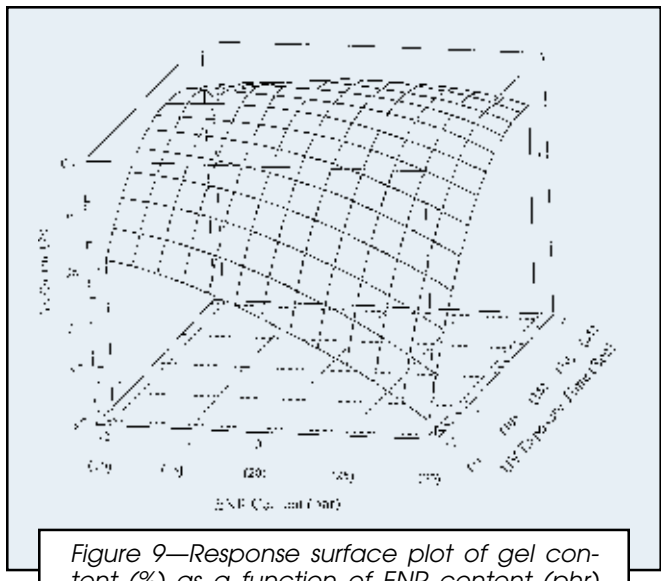


Figure 9—Response surface plot of gel content (%) as a function of ENR content (phr) and UV exposure time (sec). Values in the parentheses are the real values.

are produced concurrently with the cations. An increase in the microscopic viscosity is expected to result from increased rates of polymerizations as the photoinitiator concentration increases. This may cause viscous drag on the cations and radicals and result in their reduced diffusion rates to the reactive sites. This phenomenon can be another factor responsible for the leveling off of the hardness at higher photoinitiator concentrations.

The effect of UV exposure time on the hardness is given in *Figure 2*. It can be seen that the hardness increases as the exposure time to UV radiation increases and levels off. It should be mentioned that higher levels of surface hardness can be obtained even at lower exposure times by employing higher post-cure time or post-cure temperature.

In the present studies, interesting experimental results have been observed on the effect of process vari-

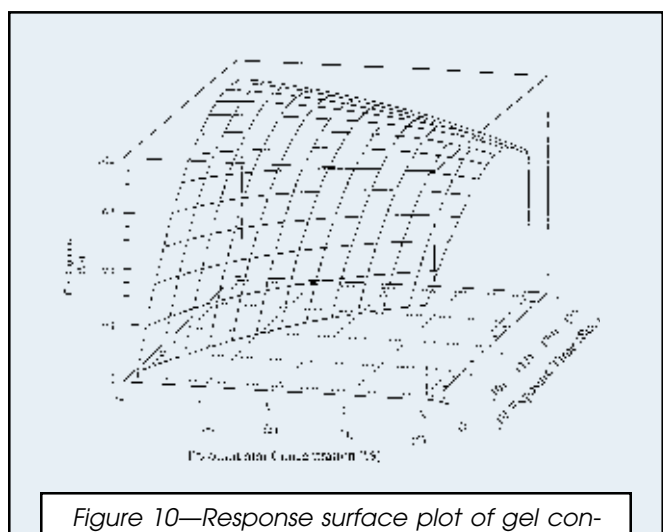


Figure 10—Response surface plot of gel content (%) as a function of photoinitiator concentration (%) and UV exposure time (sec). Values in the parentheses are the real values.

ables on the mandrel flexibility. These observations have been given in *Figures 5* to *8*. The advantages of the response surface methodology employed in the present investigation and representation of results in three-dimensional plots can be determined from these figures. From *Figures 5* and *6*, it can be seen that the flexibility increases as the ENR percentage in the formulation increases. It is also evident from the figures that a significant interaction exists between the ENR concentration and other variables, namely photoinitiator concentration (*Figure 5*), UV exposure time (*Figure 6*), post-cure time (*Figure 7*), and post-cure temperature (*Figure 8*). In other words, the effect of these process variables depends on whether the ENR concentration is at a lower value or a higher value. While the flexibility increases with increases of the previously mentioned variables at lower ENR concentration, the reverse is true at higher ENR concentration. These results are expected since the factors which would tend to increase the crosslink density would decrease the flexibility. At higher levels of ENR concentration, an increased photoinitiator concentration would bring about a higher crosslink density and hence, decreased flexibility. Another observation of noteworthy significance is the interaction between the photoinitiator concentration and post-cure temperature as given in *Figure 8*. At low levels of photoinitiator concentration, an increase in post-cure temperature has an adverse effect on the flexibility. In contrast, at higher photoinitiator concentrations, the increase of post-cure temperature increases the flexibility of the cured film. The increase in flexibility with post-cure temperature at higher photoinitiator concentrations can be attributed to the plasticizing effect of the initiator fragments remaining in the coatings.<sup>12</sup> The concentration of these fragments increases with the increase of the photoinitiator concentration.

The effects of process variables on the gel content of the film are shown in the three-dimensional plots of *Figures 9* to *11*. It can be seen from these figures that as the ENR content increases, there is a reduction in the gel content. This may be due to the increase in viscosity of the coating system at higher values of ENR content, and the rate of polymerization and crosslinking is essentially controlled by the diffusion and the viscous drag on the cations and the radicals. A recombination of the radicals in the "cage" is more likely under these conditions and the reaction zone is consequently deprived of the reactive species and the polymerization and crosslinking are adversely affected. Another interesting observation is the increase in the gel content as the UV pre-exposure time is increased as depicted in *Figure 10*.

One possible explanation could be that as the UV exposure time is increased, the surface coating system is simultaneously exposed to the infrared radiation that accompanies the UV radiation. This increases the temperature of the coating system with an initial reduction in viscosity. This reduction enables facile diffusion of the reactive species to initiate and propagate the polymerization and crosslinking reactions and hence results in an increase in the gel content. *Figure 11* gives the effect of photoinitiator concentration and post-cure temperature on the gel content. As the photoinitiator concentration increases, the gel content decreases. This may be due to

the recombination of the radicals in the cage as well as the viscous drag on the cations due to higher initial polymerization rates with the consequent increase in the local viscosity. Post-cure temperature, on the other hand, has a positive effect on the gel content as can be seen from the same figure. This may be due to the reduction of the initial viscosity of the exposed coating system which enables an easy diffusion of the reactive species to facilitate effective crosslinking reactions to occur as explained before.

**OPTIMIZATION:** The ultimate objective of response surface methodology is to determine the optimum operating conditions for the system, or to determine a region of the factor space in which desired operating specifications are satisfied. This point is called the stationary point. We wish to find the level of  $x_1, x_2, \dots, x_k$  that maximize the predicted response. This is done by partially differentiating the response equations, equating the same to zero and solving the set of simultaneous equations. The optimum conditions were obtained in coded variables for each of the responses which were converted into real variables as given in the following:

*Pendulum Hardness*—ENR content (phr):22.4; Photoinitiator (% in the formulation):1.44; UV Exposure time:13 sec; Post-cure time:60 min; Post-cure temperature:118°C

*Mandrel Flexibility*—ENR content (phr):25.5; Photoinitiator (% in the formulation):2.3; UV exposure time:23.5 sec; Post-cure time:33 min; Post-cure temperature:112°C

*Gel Content*—ENR content (phr):15.25; Photoinitiator (% in the formulation):3.72; Exposure time:17.2 sec; Post-cure time:28 min; Post-cure temperature:106°C

**CHARACTERIZATION OF THE RESPONSE SURFACE:** Geometrical representation of the response surface when more than three factors are involved is obviously complicated. This difficulty, however, can be solved since the second degree polynomial can be reduced to a standard form known as "canonical form" from which useful conclusions regarding the nature of the response surfaces and the stationary points can be drawn conveniently. The following equation represents the canonically transformed form of the fitted second degree polynomial.

$$Y - Y_s = B_{11}X_1^2 + B_{22}X_2^2 + B_{33}X_3^2 + B_{44}X_4^2 + B_{55}X_5^2$$

Where  $Y_s$  is the estimated response at the stationary point,  $B_{11}, B_{22}, B_{33}, B_{44}$ , and  $B_{55}$  are the Eigen values, and  $X_1, X_2, X_3, X_4, X_5$  are the Eigen vectors (canonical variables) of the real symmetric matrix:

$$\begin{bmatrix} b_{11} & \frac{1}{2}b_{12} & \frac{1}{2}b_{13} & \frac{1}{2}b_{14} & \frac{1}{2}b_{15} \\ \frac{1}{2}b_{21} & b_{22} & \frac{1}{2}b_{23} & \frac{1}{2}b_{24} & \frac{1}{2}b_{25} \\ \frac{1}{2}b_{31} & \frac{1}{2}b_{32} & b_{33} & \frac{1}{2}b_{34} & \frac{1}{2}b_{35} \\ \frac{1}{2}b_{41} & \frac{1}{2}b_{42} & \frac{1}{2}b_{43} & b_{44} & \frac{1}{2}b_{45} \\ \frac{1}{2}b_{51} & \frac{1}{2}b_{52} & \frac{1}{2}b_{53} & \frac{1}{2}b_{54} & b_{55} \end{bmatrix}$$

$b$ 's are the coefficients of the response function

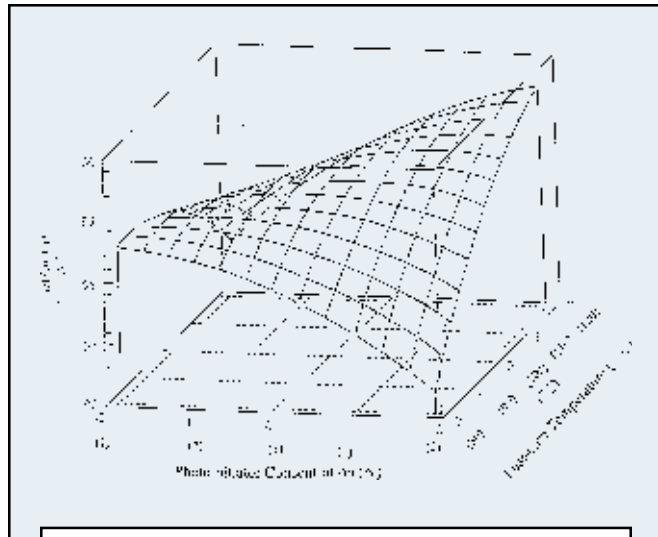


Figure 11—Response surface plot of gel content (%) as a function of photoinitiator concentration (%) and post-cure temperature (°C). Values in the parentheses are the real values.

The signs of the Eigen values help the user gain a better understanding of the response system:

- (1) If the  $B_{ii}$ 's are all negative, the stationary point is a point of maximum response.
- (2) If the  $B_{ii}$ 's are all positive, the stationary point is a point of minimum response.
- (3) If  $B_{ii}$ 's are mixed in sign, the stationary point is a saddle point.

The Eigen values for each of the responses were calculated by the Householder/Sturm method by the program described by Scraton.<sup>13</sup> These values together with their physical significance<sup>9</sup> are given in the following:

*Pendulum Hardness*— $B_{11} = -10.86158, B_{22} = -5.094528, B_{33} = -14.67706, B_{44} = -14.67706, B_{55} = 0.7933044$ .

Thus the stationary points with respect to all variables other than  $x_3$  are maxima since the Eigen values are negative. Stationary points with respect to  $x_5$  are saddle points.

*Mandrel Flexibility*— $B_{11} = -1.288216E-02, B_{22} = -0.1569972, B_{33} = 8.699775E-03, B_{44} = -0.1569972, B_{55} = -0.1569972$ .

Thus the stationary points, with respect to all variables other than  $x_3$ , are maxima since the Eigen values are negative. Stationary points with respect to  $x_3$  are saddle points.

*Gel Content*— $B_{11} = -0.726429, B_{22} = -0.4298593, B_{33} = -0.894291, B_{44} = -0.894291, B_{55} = 0.3329253$

Thus the stationary points with respect to all variables other than  $x_5$  are maxima since the Eigen values are negative. Stationary points with respect to  $x_5$  are saddle points.

## SUMMARY AND CONCLUSIONS

A set of central composite designs was investigated for three responses, namely pendulum hardness, mandrel

flexibility, and gel content. Functional relationships between the operating variables and performance properties were established using the Stagraphics software. The validity of the functional relationships was established by the ANOVA and the significance tests on the regression coefficients. The functional relationships were geometrically represented in three-dimensional response surface plots. The response surface plots enabled the physical interpretation of the results to be offered. The second order regression equation also provided the basis for the determination of optimum conditions.

## References

- (1) Kumar, R.N., Teong Jin, G., Abusamah, A., and Rozman, H.D., "Epoxy-ENR Hybrid System for Ultra-Violet Cationic Curing of Surface Coatings," Rad Tech Asia '95 Radiation Curing Conference, Guilin, China, 370-375, 1995.
- (2) Broder, M., Kordomenos, P.I., and Thomson, D.A., "A Statistically Designed Experiment for the Study of Silver Automotive Basecoat," JOURNAL OF COATINGS TECHNOLOGY, 60, No. 766, 27 (1988).
- (3) Neag, M., Wilson, P., and Skerl, G., "Coatings Characterization Using Multiple Techniques and Statistically Designed Experiments," JOURNAL OF COATINGS TECHNOLOGY, 66, No. 832, 27 (1994).
- (4) Kruithof, K.J.H. and Van den Haak, H.J.W., "A Study of Structure-Properties Relationships in Automotive Clearcoat Binders by Statistically Designed Experiments," JOURNAL OF COATINGS TECHNOLOGY, 62, No. 790, 47 (1990).
- (5) Hesler, K.K. and Lofstrom, J.R., "Combining Mixture and Independent Variables for Coatings Research," JOURNAL OF COATINGS TECHNOLOGY, 59, No. 750, 29 (1987).
- (6) Vaidya, V.S. and Nata, V.M., "Simultaneous Assessment of Influence on Hiding Power by Several Compositional Factors: Taguchi Approach," JOURNAL OF COATINGS TECHNOLOGY, 64, No. 811, 63 (1992).
- (7) Box, G.E.P., Hunter, W.G., and Hunter, J.S., *Statistics for Experimenters: An Introduction to Design, Data Analysis and Model Building*, John Wiley and Sons, New York, 1978.
- (8) Cong, D., Mon-Jun, X., Ji-Chun, Z., Wei-Pun, W., and Zue., M., *The Radiation Phys. Chem.*, 22, No. 6, 1007-1010 (1983).
- (9) Myers, R.H. and Montgomery, D.C., *Response Surface Methodology*, John Wiley & Sons Inc., 1995.
- (10) Pappas, S.P., *UV Curing: Science and Technology*, A Technology Marketing Corporation, p. 50, 1980.
- (11) Crivello, J.V., Lam, J.H.W., and Volante, C.N., *J. Rad. Curing*, 4 (3), 2 (1977).
- (12) Udagava, A., Yamamoto, Y., Inove, Y., and Chungo, R., *Polymer*, 32, No. 15, 2779 (1991).
- (13) Scraton, R.E., *Further Numerical Methods in BASIC*, Edward Arnold, 36-37, 1987.